ELSEVIER

Physica B 221 (1996) 70–76

PHYSICA B

Cu island growth on Cu(1 1 0)

I.K. Robinson*, K.L. Whiteaker, D.A. Walko

Physics Department, University of Illinois, 1110 West Green Street, Urbana, IL 61801, USA

Abstract

Submonolayer deposition of a metal upon a well-characterized surface of the same metal can be used to study the properties of surface diffusion. Satellite diffraction peaks can be observed, whose shape is related to the island size and spacing distributions. Here we present results for Cu/Cu(1 1 0) for which the temperature and rate dependencies of the resulting distributions have been examined on beamline X16A at NSLS. The results are interpreted in terms of rate-equation theories.

1. Introduction

Since the invention of the scanning tunnelling microscope (STM), there has been an explosion of interest in the question of surface morphology during growth. STM has permitted direct measurements of island shapes and sizes just after deposition of adsorbed material upon surfaces, and in between a series of depositions. Remarkable diffusion-limited-aggregation (DLA) growth forms as well as compact morphologies have been discovered in this way [1]. Considerable progress has been made at extracting diffusion barriers from such data using the STM technique [2].

While STM has led the recent progress in the field and will probably remain the primary technique for this kind of problem, there are two important experimental drawbacks that restrict the level of information that can be obtained. Firstly, it is an invasive technique that interacts strongly with the part of the system being examined; this can be avoided by moving to a fresh part of the sample after each deposit, but the measurement must always follow the deposition. Serious artifacts can arise if deposition occurs during the passage of the STM current [3]. The second limitation is that statistical average quantities are often sought for comparison with theory. Taking an ensemble average of an STM image (or multiple images) can be a painstaking operation, while a diffraction result is by definition an ensemble average over several square millimeters of sample.

Surface diffusion is the underlying physical process behind island formation during epitaxy at surfaces, and homoepitaxial systems are the most interesting to study to learn about diffusion, because hopping and exchange mechanisms are indistinguishable. It is generally recognized that the process can be broken into two distinct regimes: island nucleation and island growth. STM is particularly well suited to the island nucleation question because it measures the island density directly; diffraction methods measure lengths, therefore obtaining the density only indirectly. Some of these limitations will become apparent in this paper, which attempts to look at nucleation using diffraction. Diffraction methods may turn out to be more generally applicable in the growth regime.

Many theories of island nucleation, based on solutions of the relevant rate equations, have appeared in the

* Corresponding author.

SSDI 0921-4526(95)00907-8

literature in recent years [4–10], for which the earliest reference is to the original work of Stowell [4]. The problem is also ideal for Monte-Carlo-type simulations of which several successful studies have been accomplished. These allow valuable testing of the assumptions and can make useful predictions of the expected behavior as well [11–14]. Many of these theories introduce the concept of a critical island size, denoted i. Arriving atoms diffuse as monomers on the surface according to a diffusion equation with an activation energy E_D. They spontaneously nucleate into clusters of size j. If $j \leqslant i$, the cluster is unstable and decomposes back to monomers, but if $j > i$, the cluster becomes stable and is said to have nucleated. Clusters, once nucleated, no longer diffuse and only increase their size, and are said to enter the growth regime at this point. While the system is still in the nucleation regime (at early times), the theories predict the same generic dependence of the nucleated island density N, upon incident flux F, and temperature T:

$$N(F,T) \propto F^p \exp(E_{EFF}/kT), \tag{1}$$

where p is an exponent and E_{EFF} is some (effective) activation energy which mainly depends on the diffusion energy barrier, but also on internal binding energy of the critical nucleus. The power-law flux dependence and exponentially activated temperature dependence are strong predictions that are readily tested by experiments.

The various theories are different from each other in the interpretation of the meaning of p and E_{EFF}. For example, Venables [5,6] assigns $p = (i+1)/(i+3)$, where i is the critical nucleus size defined above, and $E_{EFF} = [E_i + (i+1)E_D]/(i+3)$ in which E_i is the binding energy of the critical nucleus and E_D is the activation energy of diffusion. This model is isotropic, but an anisotropic version was introduced by Pimpinelli et al. [5] which is most relevant to the current work on anisotropic substrates. This implicitly assumes a critical island size $i = 1$ and predicts $p = d/2(d+1)$. d is the "dimension" of the system, with $d = 1$ representing the case of one-dimensional island growth and $d = 2$ the 2D case. One-dimensional growth occurs when the diffusion can be assumed to be infinitely fast along rows in one direction, so that nucleation occurs as soon as two adjacent rows become occupied, and is therefore controlled only by hopping from row to row. In this formalism the energy appearing in the equation, E_{EFF}, is directly related to the diffusion barrier by $E_{EFF} = E_D/p$, assuming the diffusion coefficient is thermally activated.

The conventional theory is the one that has mainly been used up until now for comparison with diffraction experiments. The earliest studies of island formation were by low-energy electron diffraction (LEED) carried out on Si(1 0 0) [15]. Two more recent studies of Cu/Cu(1 0 0) have been carried out by LEED [16] and helium atom scattering (HAS) [17]. Experimental values for the exponent p were found to be 0.278–0.295 [16] and 0.23–0.27 [17], and for the effective activation energy, $E_D = 0.36$ eV [16] and $E_{EFF} = 0.07$ eV [17]. This previous experimental work utilized an isotropic substrate with 4-fold symmetry.

In this work, we consider the growth kinetics on the (1 1 0) surface of Cu, which is a simple substrate without reconstruction. The ideal clean Cu(1 1 0) surface has close-packed rows of nearest-neighbor atoms in one direction, leaving longer gaps with second-neighbor spacing, or "troughs" in the perpendicular surface direction. There is expected to be a strong anisotropy between the diffusion rates along these two orthogonal directions, which would lead to the formation of needle-like growth morphology, because islands can grow rapidly through diffusion in the "easy direction" along the troughs. The needle morphology gives rise to a diffraction intensity distribution that is mainly concentrated along a single axis, instead of being spread out in both in-plane directions. Although the diffraction from a surface is already weak, since it is diffuse along the direction of the surface normal, the anisotropy of the growth morphology makes the experiment possible. Stated another way, the Fourier transform of the needle-shaped objects, lying along the $[1\,\bar{1}\,0]$ direction of the surface plane, is a sheet of scattering, sharp in the $[1\,\bar{1}\,0]$ direction of the needle axis, but diffuse in the [1 1 0] direction of the surface normal as well as in the [0 0 1] in-plane direction.

The needle morphology has been seen by STM for the closely related system Cu/Pd(1 1 0) [18]. The temperature dependence of the 1D and 2D island densities was measured in this way and interpreted by using Eq. (2). The aspect ratio of the islands was found to be temperature dependent as well. Diffusion barriers of $E_{D,001} \approx 0.75$ eV and $E_{D,1\bar{1}0} \approx 0.51$ eV were obtained for the two orthogonal directions across the surface [18].

In this diffraction experiment, we can ignore the dependence of the profile on the perpendicular momentum transfer along [1 1 0], and concentrate on its shape along the in-plane directions, [0 0 1] and $[1\,\bar{1}\,0]$, which is directly related to the island size and spacing distributions. This assumes we are always working in the submonolayer regime. If, for example, the islands were uniformly spaced with separation d, the diffraction pattern would be that of a grating, or an array of satellite peaks displaced by multiples of $2\pi/d$. It is more likely that the spacing will be irregular, but not altogether random, so there will be a distribution of spacings centered around some typical value d_{AVE}; the diffraction will be broad but still peaked at positions $2\pi n/d_{AVE}$.

This picture is complicated further when the size distribution of the islands is included as well as that of the spacing. Diffraction profiles have been calculated for

Monte Carlo simulations of growth morphologies [14], but unfortunately only in the 2D isotropic case. A general formalism for calculating the diffraction profile from general size-distribution and spacing-distribution functions has also been developed [19], and we plan to use that ultimately for fitting of the data [20]. In the meantime, we simplify the analysis by working only at half-monolayer coverage, $\theta = 0.5$ ML, under which conditions the size of the islands should be equal to size of the spaces between the islands. It follows that the diffraction line shape may be expected to be characterized by a single length scale. More complicated analysis will probably be needed for cases with $\theta \neq 0.5$ ML.

2. Experimental method

The experiments were carried out on beamline X16A at the National Synchrotron Light Source (NSLS) in a customized ultra-high vacuum (UHV) X-ray diffractometer [21]. The Cu(1 1 0) crystal was cleaned by sputtering and annealing, then cooled to the growth temperature, T, on a liquid-nitrogen-cooled manipulator. Cu was deposited from a graphite crucible with a small aperture (Knudsen cell), for which the temperature T_{source} determined the deposition rate. The crystal was aligned by means of its bulk $\{1\,1\,1\}$ and $\{2\,0\,0\}$ reflections, and measurements of the surface were made on the $(0, 1, L)_{\text{SURFACE}}$ crystal truncation rod (CTR) at $L \approx 0.08$, close to its midpoint at $L = 0$ for good surface sensitivity [22]. To enhance signal to background, the incidence angle β was controlled to be 0.4°, close to the critical angle for total external reflection at 8.5 keV. Scans were made mainly along the in-plane direction $(h, 1, 0.08)_{\text{SURFACE}}$, where h is the reciprocal lattice coordinate along the FCC [0 0 1] direction, as defined above. These data are therefore sensitive to the distribution of island spacings and sizes across their narrow direction, and do not probe information along the direction of the needle morphs. When distinct side peaks were detected their width was also measured with corresponding k-scans.

3. Results

Two examples of h-scans are shown in Fig. 1. Both were made after $\theta = 0.5$ ML of Cu was deposited at a flux of 4×10^{-3} ML/s. Only the sample temperature was changed between the two measurements. The half-monolayer coverage point was determined by extrapolating the initial slope of the CTR intensity versus time plot to zero, as would correspond to ideal parabolic dependence. The remaining intensity at this point was then less than

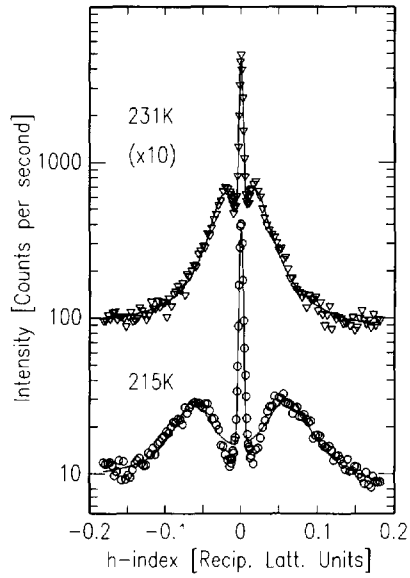

Fig. 1. Transverse scans of Cu(1 1 0) with a 0.5 ML deposit of Cu measured along $(h, 1, 0.08)$ at the same flux but two different sample temperatures. Fit curves are superimposed for a sum of a single Gaussian (center) and two Lorentzians (sides). The line shape has a clear asymmetry which is not properly fit by this approximate functional form.

20% of its initial value. The remains of the sharp central CTR peak and the side lobes are clearly visible in both cases, the latter indicating a clearly preferred spacing of the islands, d_{AVE}. This spacing also depends strongly upon the substrate temperature during the growth. The side-peak line shape is clearly asymmetric about its center, with a long tail on the outer side. In the interim, before detailed fitting of these curves becomes available [20], we have simply used a line shape consisting of the sum of a Gaussian and two Lorentzians to estimate the side-peak positions and widths, as shown.

The first conclusion we can derive from such data is that the $\theta = 0.5$ ML distribution function scales with substrate temperature. This can be seen directly from the data, without a need to know its actual distribution function, by transforming the data to normalize the height, width and background of the side peaks. Such a "data collapse" is shown in Fig. 2, with four temperature points superimposed. At the level of the statistics, the curves are the same, indicating the same functional form for the size distribution. The mosaic-limited central CTR peak is seen to peel off from the rising edge of the line shape at different places, as it should because this component does not rescale. The diffraction function is most clearly separated from the central peak at the lowest temperatures, but the statistics there are the worst.

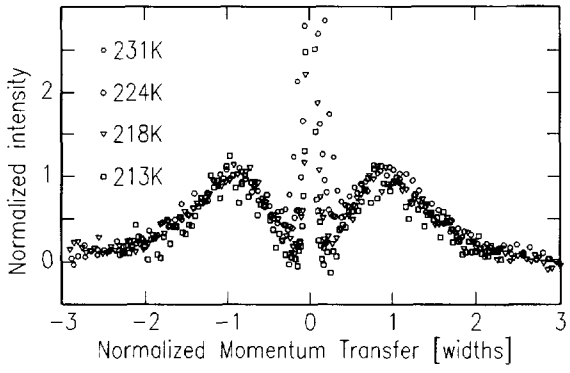

Fig. 2. Demonstration of scaling of the data in Fig. 1 by normalization of both horizontal and vertical axes. The same island size distribution function is suggested for all four temperatures shown.

Even though the fitting is imperfect and does not explain the asymmetry of the side peaks, the fit parameters are nevertheless representative of the island sizes and spacings. This is only true because the functional form of the peaks is conserved, as we demonstrated above, so the effect of distortions will be the same at all temperatures. As explained above, if the side-peaks appear at positions $\pm h_{MAX}$, this provides the average spacing between the islands,

$$d_{AVE} = a_0/|h_{MAX}|,$$

where a_0 is the unit cell dimension along [0 0 1], which is equal to the lattice constant of Cu, 3.615 Å. Similarly the half-width at half maximum (HWHM) of the entire peak is representative of the average island size along [0 0 1]. This can be written in terms of the Lorentzian peak position, h_{MAX}, and its half-width in the h-direction, Δh_{HWHM},

$$L_{001} = 0.367 a_0/(\Delta h_{HWHM} + |h_{MAX}|),$$

where the numerical constant is determined by finding the best fit of a Lorentzian to a slit function, which is the Fourier transform in 1D of a block of length L. If a Gaussian-distributed object with full-width at half maximum, L, had been considered, the numerical factor relating the HWHM of the resulting Gaussian would have been 0.312 instead, so the actual value is not very sensitive to the details of the line shape.

If the line shape scaled perfectly with flux and temperature, as Fig. 2 suggests, the values of L_{001} and d_{AVE} would be proportional to each other, and all information about the width of the distribution would be carried by either one. Even though the side peaks appear to scale quite well, there is considerable overlap with the central maximum, which distorts our fit to simple functions and leads to significant perturbations in the resulting fit parameters. We would expect the overall width to be less sensitive to this distortion than d_{AVE}, but will nevertheless keep track separately of d_{AVE} and L_{001} in the subsequent discussion, even though they should represent the same thing.

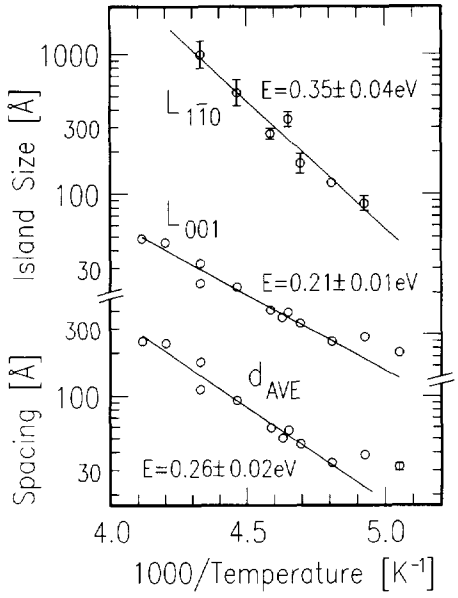

Fig. 3. Substrate temperature dependence of the line shape fitting parameters in the form of an Arrhenius plot. The measurements each correspond to separate depositions at the same flux of 4×10^{-4} ML/s. The island size parameters, L_{001} and $L_{1\bar{1}0}$, are obtained from the widths of the side peaks (see text), in the transverse and radial directions, respectively. The spacing, d_{AVE}, is derived from the positions of the side peaks. The slopes of the lines are activation energies, and were evaluated by a linear regression.

Measurements along the radial k-direction through the side peaks at $(\pm h_{MAX}, 1, 0.08)$ were found to be significantly broader than resolution for growth experiments below 230 K, and were reasonably well fit with a Lorentzian line shape of half-width Δk_{HWHM}. This suggests that the islands are uncorrelated along k, and it follows that the peak width is determined only by the island size in this direction. After deconvolution of resolution (by direct subtraction), the average island length along $[1\bar{1}0]$ can be determined by

$$L_{1\bar{1}0} = 0.367/\sqrt{2}\, a_0/\Delta k_{HWHM}.$$

The temperature dependencies of the three quantities, d_{AVE}, L_{001} and $L_{1\bar{1}0}$ are shown together in Fig. 3 in the form of an Arrhenius plot, and their flux dependencies are shown at two different temperatures in Figs. 4 and 5 as log–log plots.

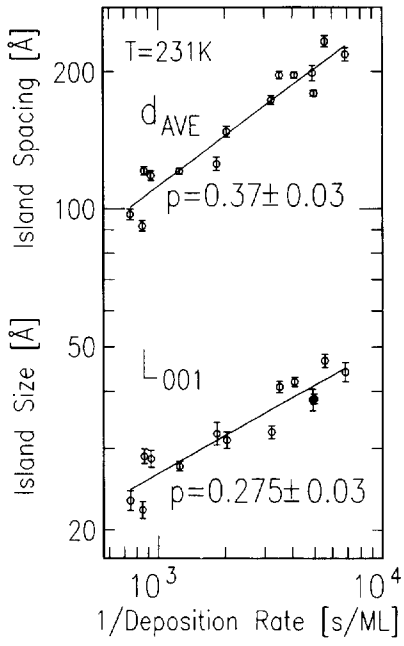

Fig. 4. Flux dependence of the island spacing, d_{AVE}, and the island sizes L_{001} measured at a sample temperature of 231 K. The flux was measured experimentally for each point from the time dependence of the CTR central peak intensity. A log–log plot is used to determine the flux exponents, which have values 0.37 ± 0.03 for d_{AVE} and 0.275 ± 0.03 for L_{001}.

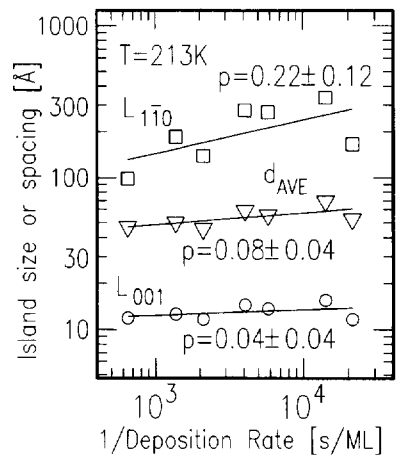

Fig. 5. Flux dependence of the island sizes $L_{1\bar{1}0}$ and L_{001} and their spacing, d_{AVE}, measured at a sample temperature of 213 K. The exponents (slopes) have values 0.22 ± 0.12 for $L_{1\bar{1}0}$, 0.08 ± 0.04 for d_{AVE} and 0.04 ± 0.04 for L_{001}.

4. Discussion

The strong temperature dependence and milder flux dependence of the island morphology arises because of diffusion rates of atoms across the surface. The theories of nucleation mentioned above [4–10] are based on solving rate equations and therefore directly address the rate of nucleation, or the density of nuclei formed after a certain time. Diffraction measurements are most useful at determining the sizes of microscopic objects, and cannot be used directly to monitor island density. Any theory that applies to the growth regime will indeed predict island sizes as a function of time, but at present this is available mainly from Monte Carlo simulations [11–14] in the form of island size distributions. At present, these exist only for isotropic substrates, and comparison of our data even with these will require a more detailed analysis, which is still in progress [20].

We can nevertheless make a simple comparison with the rate-equation theories [4–10] by making certain assumptions about the relationship between the average island density and the island sizes:

$$N_{2D}(F, T) \propto \theta / L_{001} L_{1\bar{1}0}, \tag{2}$$

$$N_{1D}(F, T) \propto \theta / L_{001}. \tag{3}$$

Noting that the generic form of Eq. (1) applies to a wide range of nucleation theories, we can use Eqs. (2) and (3) to fit the data for the F-dependence and T-dependence of L_{001} and $L_{1\bar{1}0}$, to estimate the exponent p and the effective activation energy E_{EFF}. These parameters can then be related to the specific microscopic quantities relevant to the individual theories, as explained above. In particular, the anisotropic ($d = 1$), smallest critical island size ($i = 1$) rate-equation theory [7] predicts $p = \frac{1}{4}$.

The exponent p is determined from the flux dependence (Figs. 4 and 5). The side peak width along $1\bar{1}0$ is resolution-limited at the higher temperature, 231 K, so a determination of p based on $L_{1\bar{1}0}$ is not possible from Fig. 4, and so we cannot use Eq. (2) either. However we do have data on d_{AVE} and L_{001}: the exponent for the first of these, 0.37 ± 0.03, is higher than expected, but the second, 0.275 ± 0.03, is within error of the 1D expected value of $p = \frac{1}{4}$. We believe this supports our expectation that L_{001} would be a more representative quantity than d_{AVE}.

At 213 K in Fig. 5, the value of the N_{2D} exponent in Eq. (2) is given by the sum of the slopes of the log–log fits for L_{001} and $L_{1\bar{1}0}$. This gives $p = 0.26 \pm 0.12$, which is consistent with $p = \frac{1}{4}$ or $p = \frac{1}{3}$ because it is so poorly determined. Once again d_{AVE} is found to give a larger exponent than L_{001}. $p = \frac{1}{3}$ is the value expected for $d = 2$, $i = 1$ [7]. However, it appears from Fig. 3 that 213 K (4.7×10^{-4} K^{-1}) is the temperature at which

diffusion along [0 0 1] ceases to be thermally activated (see below), so the exponent determined there may be invalid anyway. Even if this were true, diffusion along [1 $\bar{1}$ 0] is still active and the exponent of 0.22 ± 0.12 measured for $L_{1\bar{1}0}$ may still be meaningful, as it is indeed consistent with $p = \frac{1}{4}$ for N_{1D} in Eq. (3). Perhaps more importantly, both our exponent values at 231 and 213 K are also consistent with previous experimental values (albeit on an isotropic substrate) of 0.23–0.27 [17] and 0.278–0.295 [16].

The activation energies are obtained from the temperature dependence, which is shown in Fig. 3. The slopes of the Arrhenius plots are $E = 0.26 \pm 0.02$ eV for d_{AVE}, $E_{001} = 0.21 \pm 0.01$ eV for L_{001} and $E_{1\bar{1}0} = 0.35 \pm 0.04$ eV for $L_{1\bar{1}0}$. If we accept the assumption of a critical nucleus size, $i = 1$, we mentioned above that the slope E_{EFF} does not depend on any binding energy and so should be identified with $2E_D(d + 1)/d$ [7], or $4E_D$ when $d = 1$. $E_{001} = 0.21 \pm 0.01$ eV then gives $E_{D,001} = 0.84 \pm 0.04$ eV for the diffusion barrier along [0 0 1]. If the nucleation is indeed one-dimensional, the meaning of the apparent thermal activation of $L_{1\bar{1}0}$ and the resulting $E_{1\bar{1}0} = 0.35 \pm 0.04$ eV must correspond to some other mechanism, such as edge diffusion on already nucleated islands, or some modification during the growth of the nucleated islands up to 0.5 ML. We consider it unlikely that $E_{1\bar{1}0}$ is related to $E_{D,1\bar{1}0}$ (in the same way as the [0 0 1] quantities) because it would imply a bigger activation energy for diffusion along the rows than across, which violates common sense: diffusion barriers should be smaller along the troughs of a 1 1 0 surface, where fewer nearest neighbor bonds must be broken, than across them.

Typical theoretical predictions of diffusion barriers, based on effective medium theory for Cu(1 1 0), are $E_{D,001} = 0.83$ eV and $E_{D,1\bar{1}0} = 0.29$ eV [23]. The first number is in excellent (perhaps fortuitous) agreement with our determination. The barrier for Cu/Pd(1 1 0) determined by STM [18] is $E_{D,001} = 0.75 \pm 0.07$ eV, also in good agreement. Rather than comparing with theory, a direct comparison of our data with the STM data for Cu/Pd(1 1 0) [18] is possible. No STM flux dependence is published, but the temperature data extend higher than our resolution limit permits measurement. The T-dependence of the 1D island density agrees well with our data for L_{001}, including the flattening of the curve seen at low T in Fig. 3, which is interpreted as a crossover between 1D and 2D growth in Ref. [18]. The temperature scale is different: the inflection occurs at 210 K for Cu/Cu(1 1 0) but 300 K for Cu/Pd(1 1 0). There is quantitative agreement in the data for the aspect ratio, $L_{001}/L_{1\bar{1}0}$, of the islands between 210 and 250 K, but this may be coincidental since this range is below the inflection temperature for Pd(110) and above it for Cu(1 1 0).

5. Conclusion

We have shown that a limited amount of information about island nucleation can be obtained using X-ray diffraction by observing the resulting island's average dimensions once the total coverage has grown to 0.5. The exponents and activation energies for diffusion of Cu on Cu(1 1 0) obtained in this way are consistent with the expectations of nucleation theories based on rate equations. We observe a strongly activated dependence of the island size along [1 $\bar{1}$ 0] that must be due to some other mechanism than nucleation. In addition, we have measured the resulting island size distributions after growth to $\theta = 0.5$ that can be compared with the expectations of Monte Carlo simulations when they become available for an anisotropic substrate [20].

Acknowledgements

We thank R. Schuster for help in the experimental stages of the early part of this work, and K. Kern for valuable discussions. These activities on beamline X16A are supported by NSF DMR 93-15691. NSLS is supported by DOE contract DE-AC02-76CH00016.

References

[1] R.Q. Huang, J. Schröder, C. Günther and R.J. Behm, Phys. Rev. Lett. 67 (1991) 3279.
[2] H. Brune et al., Phys. Rev. Lett. 73 (1994) 1955.
[3] J. Lagraff and A.A. Gewirth, J. Chem. Phys. 98 (1994) 11246.
[4] M.J. Stowell, Phil. Mag. 21 (1970) 125.
[5] J. Venables, Phil. Mag. 27 (1973) 693.
[6] J. Venables, G.D.T. Spiller and M. Hanbücken, Rep. Prog. Phys. 47 (1984) 399.
[7] A. Pimpinelli, J. Villain and D.E. Wolf, Phys. Rev. Lett. 69 (1992) 985.
[8] M.C. Bartelt and J.W. Evans, Phys. Rev. B 46 (1992) 12675.
[9] J. Villain, A. Pimpinelli, L. Tang and D. Wolf, J. Phys. I France 2 (1992) 2107.
[10] J. Villain, A. Pimpinelli and D.E. Wolf, Comments Cond. Matt. Phys. 16 (1992) 1.
[11] G.S. Bales and D.C. Chrzan, Phys. Rev. B 50 (1994) 6057.
[12] C. Ratsch, A. Zangwill, P. Smilauer and D.D. Vvedensky, Phys. Rev. Lett. 72 (1995) 3217; C. Ratsch, A. Zangwill and P. Smilauer, Surf. Sci. Lett. 314 (1994) L937.
[13] J.G. Aamar and F. Family, Phys. Rev. Lett. 74 (1995) 2066.
[14] M.C. Bartelt and J.W. Evans, Surf. Sci. 298 (1993) 421.

[15] P. Hahn, J. Clabes and M. Henzler, J. Appl. Phys. 51 (1980) 2079.
[16] J.K. Zuo, J.F. Wendelken, H. Dürr and C.L. Liu, Phys. Rev. Lett. 72 (1994) 3064; H. Dürr, J.F. Wendelken and J.K. Zuo, Surf. Sci. 328 (1995) L527.
[17] H.J. Ernst, F. Fabre and J. Lapujoulade, Phys. Rev. B 46 (1992) 1929.
[18] J.P. Bucher, E. Hahn, P. Fernandez, C. Massobrio and K. Kern, Europhys. Lett. 27 (1994) 473.
[19] J.M. Pimbley and T.M. Lu, J. Appl. Phys. 57 (1985) 1121; J.M. Pimbley and T.M. Lu, J. Appl. Phys. 58 (1986) 2184.
[20] D.A. Walko, K.L. Whiteaker and I.K. Robinson, to be published.
[21] P.H. Fuoss and I.K. Robinson, Nuclear Instr. Methods 222 (1984) 171.
[22] I.K. Robinson, Phys. Rev. B 33 (1986) 3830.
[23] P. Stolze, J. Phys.: Condens. Matter 6 (1994) 9495.